ROTATING SENSOR-MATRIX CAMERA CALIBRATION

Fay Huang, Reinhard Klette+, Yin-Wei Chang*, and Tien-Ju Chi**

* National Ilan University, Institute of Computer Science and Information Engineering
Yi-Lan, Taiwan
+ The University of Auckland, Computer Science Department
Auckland, New Zealand

ABSTRACT

Panoramic images and panoramic cameras (or sensors) are of increasing importance for various applications in computer vision, computer graphics, visualization, and robotics. Various panoramic image capturing sensors have been developed for different purposes. But many of the sensing devices do not support stereo visualization. This paper reviews a methodology for stereo panorama acquisition using a widely available digital matrix camera. We also propose a method for camera calibration. The calibration process of such an image acquisition system is essential to ensure a high quality of stereo visualization.

Index Terms— Panoramic Imaging, Stereo Panorama, Camera Calibration

1. INTRODUCTION

Panoramic images have been widely used in 3D scene visualization, navigation and reconstruction applications. A 360-degree cylindrical panorama records scene information of all possible viewing directions at a single viewpoint, which supports the capability of wide-angle displaying. It gained its popularity in public exhibition galleries, museums, showrooms, or theaters, as well as for web-based visualization of environments such as in Google Map.

Over the last few years, various stereoscopic visualization and display technologies have become more and more accessible and affordable to end-users. Panoramic image applications have also started to provide stereo visualization. As a result, the research topics related to stereo panoramic image acquisition, analysis and visualization have received an increasing interest. Stereo panoramic images have been used for robot navigation [8], 3D scene understanding and reconstruction [7, 3], environmental documentation [5], and, of course, for stereo visualization in various types of virtual reality systems [1] or stereo photography [4].

In the paper, we recall at first a relatively new methodology for accurate stereo panorama acquisition, called a rotating sensor-line camera [2], which is capable of not only capturing a stereo panorama but is also able to preserve the geometrical accuracy of the 3D scene information within the images. The only shortage of such a camera is a relatively high image acquisition time for a 360-degree scan. We discuss in the paper then an alternative approach based on a (standard) sensor-matrix camera, which is able to capture stereo panoramas more effectively, but with a trade-off between speed and accuracy. For applications such as entertainments and virtual reality, this alternative approach would be sufficient.

The main contribution of the paper is the proposed camera calibration method for a rotating sensor-matrix camera. The accurate recovery of the camera parameters is very important to ensure a high quality stereo visualization of the resulting stereo panorama and an accurate camera pose estimation from multiple panoramas.

2. CAMERA GEOMETRY

This section introduces the imaging geometry and notation as used in this paper.

2.1. Rotating Sensor-line Cameras

A digital camera equipped with a linear sensing element (e.g., a single column CCD) is placed on a tripod and rotated, taking many images, "column by column", during such a rotation. This defines a *rotating sensor-line camera*, which is capable of recording a 360° panoramic images with very high image resolution. Figure 1 demonstrates an example of a high-resolution panorama captured by a rotating sensor-line camera. The resolution of this panorama is 56,580 × 10,200 pixels, and the size of the image is 3 GB.

Rotating sensor-line cameras (see Figure 2) have been the subject of the book [2]. We use the same notation as in this book, which provided a general model for rotating sensor-line cameras. The intrinsic camera parameters, R (radius of base circle, also called off-axis distance), f (focal length of camera) or g for a projection parameter in general, and ω (principle angle) characterize how a panoramic image is acquired.

Fig. 1. A high-resolution panoramic image of Auckland city from the top of the Harbour Bridge, captured in 2001.

2.2. Rotating Sensor-Matrix Cameras

A sensor-matrix camera is more accessible and lower in price then a sensor-line camera. Thus, an alternative panoramic image acquisition would be by rotating a normal matrix camera on a tripod instead of using a line camera. The final panoramic image is generated by combining some particular image columns of each shot. Thus, the geometry is very much similar to the imaging geometry of a rotating line camera. In order to reduce the panoramic image acquisition time, normally a set of adjacent image columns are used for each shot to generate the panoramic image. Consequently, less shots are required during a full rotation. Figure 3 illustrates an example of a stereo panorama captured by a rotating sensor-matrix camera.

We unify the notations between both approaches by conversions as described below. According to the definition of a model of a rotating sensor-line camera, any column of the sensor-matrix defines one specific panoramic image; see left of Fig. 4. The choice of the column corresponds to the choice of angle ω, and every column identifies a different projection parameter g (note: we only have $g = f$ for one sensor-column $c_{\mathcal{M}}$ where the optical axis of the camera passes through).

Let ψ be the angle between the surface normal of the sensor-matrix and the normal of the base circle (at a given position of the camera **C**) as shown in Fig. 4, right. The panorama composed by the ith column of the sensor matrix has the following parameter values: R remains unchanged; the values of the projection parameter and the principle angle

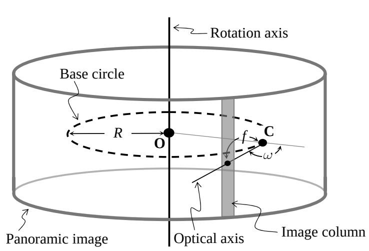

Fig. 2. Basic entities of a rotating sensor-line camera.

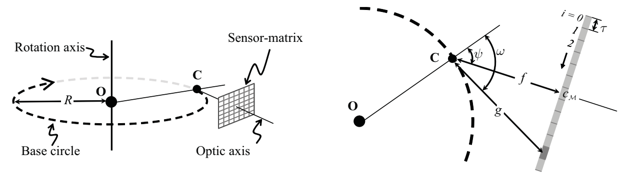

Fig. 4. Left: A rotating sensor-matrix camera. Right: Illustration for the notation conversions.

are calculated as

$$g = \sqrt{f^2 + (i - c_{\mathcal{M}})^2\,\tau^2} \quad \text{and} \quad \omega = \psi + \arctan\left(\frac{(i - c_{\mathcal{M}})\,\tau}{f}\right)$$

respectively, where τ is the size of a single sensor-cell (assuming perfectly square pixel) and f is the focal length of the camera.

For this system, an off-axis distance (i.e., $R > 0$) together with the principle angle ω offer the capability of acquiring stereo panoramas. A stereo panorama can be acquired at a single location with constant values of R, but for two different (symmetric) values ω and $-\omega$. (Note that these two values are symmetric with respect to the normal of the base circle.) Such a pair of panoramas is directly stereo viewable [6] because any pair of corresponding points lies on the same image row. The major task of the paper is to calibrate these two important camera parameters R and ω.

3. CAMERA CALIBRATION

Intrinsic parameters of the camera used for panoramic image acquisition can be accurately calibrated in advance using some publicly available toolbox. Thus, the focal length f (in pixel) and the central row j_c are assumed to be known. The task here is to calibrates the off-axis distance R and principle angle ω of our camera setup. We present a *parallel line approach* that uses geometric properties of parallel line segments (calibration lines) available in the scene. It is a standard procedure to ensure that both the camera and the rotating rig are both leveled during image acquisition. Therefore, we aim to use vertical edges available in the scene to recover the sensor parameters. The advantage of this approach is that no calibration object is needed.

We assume that there are at least three pairs of parallel straight line segments in the scene (e.g., straight edges of doors or windows), which are parallel to the rotation axis. For each straight line segment we further assume that both endpoints are visible (from the camera) and identifiable in the panoramic image, and that we may have an accurate measurement of the physical distance between these two end points. Finally, we assume that the distances between selected pairs of parallel lines are also measurable and known.

Any useable straight line segment in the 3D scene is denoted as $\mathcal{L}$ and indexed where needed for the distinction of

Fig. 3. Anaglyphic stereo panorama of Ilan University captured in 2007.

multiple lines. The (Euclidean) distance of two visible points on a line $\mathcal{L}$ is denoted by H. The length of a projection of a line segment on an image column is denoted by h and measured in pixel. Examples of H_k and corresponding h_k are illustrated in Figure 5, where $k \in [1, \ldots, 5]$. Let D_{ij} denote the distance between two parallel lines $\mathcal{L}_i$ and $\mathcal{L}_j$. If the distance between two straight line segments is available then we say that both lines form a *pair of lines*. A line segment may be paired up with more than just one other line segment.

Consider a pair of lines $\mathcal{L}_i$ and $\mathcal{L}_j$ in 3D space. The angular distance of two image columns, associated to these two lines, is the angle $\angle \mathbf{C}_i\mathbf{O}\mathbf{C}_j$, where $\mathbf{O}$ is the center of the base circle and $\mathbf{C}_i$ and $\mathbf{C}_j$ are the corresponding optical centers (which "see" this line segment). We denote the angular distance of a pair ($\mathcal{L}_i$, $\mathcal{L}_j$) of lines by θ_{ij}. An example of angular distance for pairs of lines is given in Fig. 5, right. The distance S between a line segment $\mathcal{L}$ and the associated optical center can be obtained by equation $S = \frac{gH}{h}$, where g is the pre-calibrated projection parameter corresponding to this panoramic image.

3.1. Geometric Relation

Now we are ready to formulate a distance constraint by combining all the previously described geometric information. A 2D coordinate system is defined on the base plane for every pair of lines ($\mathcal{L}_i$, $\mathcal{L}_j$); see right of Figure 5. Note that even though all the measurements are defined in 3D space, the geometric relation of interest can be described in a 2D space since all the straight segments are assumed to be parallel to the rotation axis. The origin of the coordinate system is $\mathbf{O}$, and the Z-axis is incident with the camera focal point $\mathbf{C}_i$. The X-axis is orthogonal to the Z-axis and is incident with the base plane.

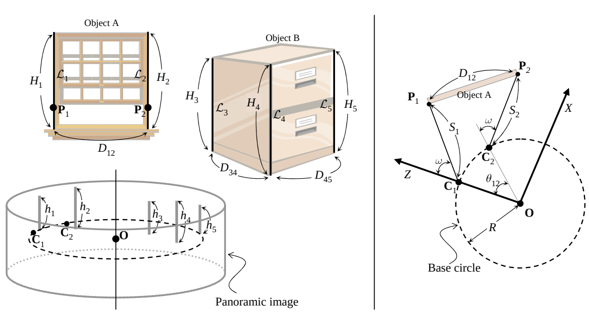

Fig. 5. Left: Configurations of parallel straight lines in the 3D scene and on the panoramic image. Right: A defined coordinate system for any pair of lines (from top view).

The position of $\mathbf{C}_i$ can now be described by coordinates $(0, R)$, and the position $\mathbf{C}_j$ can be described by coordinates $(R\sin\theta_{ij}, R\cos\theta_{ij})$. The intersection point of line $\mathcal{L}_i$ with the base plane, denoted as $\mathbf{P}_i$, can be expressed by a sum of vector $\overrightarrow{\mathbf{OC}_i}$ and vector $\overrightarrow{\mathbf{C}_i\mathbf{P}_i}$. Thus, we have the following:

$$\mathbf{P}_i = \begin{bmatrix} S_i \sin\omega \\ R + S_i \cos\omega \end{bmatrix}$$

Analogously, the intersection point of line $\mathcal{L}_j$ with the base plane, denoted as $\mathbf{P}_j$, can be described by a sum of vectors $\overrightarrow{\mathbf{OC}_j}$ and $\overrightarrow{\mathbf{C}_j\mathbf{P}_j}$. We have the following:

$$\mathbf{P}_j = \begin{bmatrix} R\sin\theta_{ij} + S_j \sin(\theta_{ij} + \omega) \\ R\cos\theta_{ij} + S_j \cos(\theta_{ij} + \omega) \end{bmatrix}$$

The distance D_{ij} between points $\mathbf{P}_i$ and $\mathbf{P}_j$ has been measured. We have the following equation:

$$\begin{aligned} D_{ij}^2 &= (S_i \sin\omega - R\sin\theta_{ij} - S_j \sin(\omega + \theta_{ij}))^2 \\ &+ (R + S_i\cos\omega - R\cos\theta_{ij} - S_j\cos(\omega + \theta_{ij}))^2 \end{aligned} \quad (1)$$

3.2. Error Function

Basically we use Equation (1) as error function. The values of S_i, S_j, D_{ij}, and θ_{ij} are known. Thus, Equation (1) can be arranged into the linear form $A_1X_1 + A_2X_2 + A_3X_3 + A_4 = 0$ with coefficients A_n, $n = 1, 2, 3, 4$, defined as follows:

$$\begin{aligned} A_1 &= 1 - \cos\theta_{ij} \\ A_2 &= (S_i + S_j)(1 - \cos\theta_{ij}) \\ A_3 &= -(S_i - S_j)\sin\theta_{ij} \\ A_4 &= \frac{S_i^2 + S_j^2 - D_{ij}^2}{2} - S_iS_j\cos\theta_{ij} \end{aligned}$$

For the three linearly independent variables X_n, $n = 1, 2, 3$, we have $X_1 = R^2$, $X_2 = R\cos\omega$, and $X_3 = R\sin\omega$.

In this case we can solve for values R and ω by using all three equations. If more than three equations are provided then it is possible to apply a linear least-square technique. To tackle the multiple-solution problem, we constrain the parameter estimation process further by $X_1^2 = X_2^2 + X_3^2$.

Assume that N copies of Equation (1) are given. We want to minimize the following:

$$\sum_{n=1}^{N} (A_{1n}X_1 + A_{2n}X_2 + A_{3n}X_3 + A_{4n})^2 \quad (2)$$

Fig. 6. The panoramic image for camera calibration.

subject to the equality constraint $X_1 = X_2^2 + X_3^2$, where the values of A_{1n}, A_{2n}, A_{3n}, and A_{4n} are calculated based on measurements in the real scene and in the image. Now, the values of R and ω can be uniquely (!) calculated as

$$R = \sqrt{X_1} \quad \text{and} \quad \omega = \arccos\left(\frac{X_2}{\sqrt{X_1}}\right)$$

Note that even though the additional constraint forces a use of a non-linear optimization method, the accuracy of the method remains at the quality level of a linear parameter estimation procedure.

4. EXPERIMENTS

Real and synthetic experiments were conducted to evaluate the proposed method. The synthetic experiments were carried out using *3D Max*, where the ground truth values of all the parameters were known. Grid patterns were mapped on the walls in the virtual environment and captured by a virtual camera. We had $R = 0.5$ m, $\omega = 60°$, and $g = 1555.5$ pixel, and the image resolution was 3,600 $\times$ 1,600. The generated panoramic image is shown in Fig. 7. Ten pairs of parallel lines (highlighted in red) were used for calibration, and we obtained $R = 0.5054$ m and $\omega = 60.2991°$. The minor deviations of recovered values compared to the true values were caused by rounding-off error of endpoint pixel identifications.

The real-image experiments were performed indoor; the parallel lines used for calibration are shown in Fig. 6. The lengths of those line segments were within the range of 0.5 m to 1.2 m and were measured with an error of less than 0.005 m. The camera was set up as accurate as possible, such that we had $R = 0.5 \pm 0.01$ m and $\omega = 60 \pm 1°$. The sensor-matrix camera was accurately pre-calibrated and we had $g = 3133.57$ pixel. The recovered values of R and ω based on our approach were 0.5117 m and $59.7786°$. The results are about as accurate as the synthetic experiment. We conclude that the proposed camera calibration method is practical because errors are reasonably small.

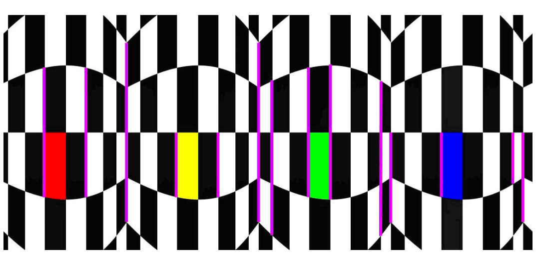

Fig. 7. A synthetic panorama for camera calibration.

5. CONCLUSIONS

This paper reviewed the methodology for stereo panorama acquisition using either a sensor-line or a widely available sensor-matrix camera. A camera calibration approach for recovering two essential parameters of the system, off-axis distance and principal angle, were presented. The calibration can be performed anywhere as long as there are more than three pairs of vertical parallel lines available in the scene. Both the synthetic and real experiments showed that the proposed method is able to achieve good accuracy even if there are errors introduced by measurements and pixel identifications.

6. REFERENCES

[1] C.-W. Chen, L.-W. Chan, Y.-P. Tsai, and Y.-P. Hung. Augmented stereo panoramas. In Proc. *ACCV*, LNCS 3851, pages 41–49, 2006.

[2] F. Huang, R. Klette, and K. Scheibe. *Panoramic Imaging: Sensor-Line Cameras and Laser Range-Finders*. Wiley, Chichester, U.K., 2008.

[3] W. Jiang, M. Okutomi, and S. Sugimoto. Panoramic 3D reconstruction using rotational stereo camera with simple epipolar constraints. In Proc. *CVPR*, Volume 1, pages 371–378, 2006.

[4] M. Murakami. StereoMaker and stereo panoramas. Available: `http://www.stereomaker.net/eng/`, 2006.

[5] NASA, STEREO project. Available: `http://www.nasa.gov/mission_pages/stereo/main/`, 2007.

[6] S. Seitz and J. Kim. The space of all stereo images. *Int. J. Computer Vision*, 48:21–38, 2002.

[7] H.-Y. Shum and R. Szeliski. Stereo reconstruction from multiperspective panoramas. In Proc. *Int. Conf. Computer Vision*, pages 14–21, 1999.

[8] W. Stürzl and H.A. Mallot. Vision-based homing with panoramic stereo sensor. In Proc. *BMCV*, LNCS 2525, pages 620–628, 2002.